Short-Pulse Laser Damage in Transparent Materials as a Function of Pulse Duration

An-Chun Tien, Sterling Backus, Henry Kapteyn, Margaret Murnane, and Gérard Mourou

University of Michigan, Center for Ultrafast Optical Science, 2200 Bonisteel Boulevard, Ann Arbor, Michigan 48109-2099

(Received 24 September 1998)

We present a single-shot damage threshold measurement and modeling for fused silica at 800 nm as a function of pulse duration down to 20 fs. We examine the respective roles of multiphoton ionization, tunnel ionization, and impact ionization in laser damage. We find that avalanche predominates even in the case of sub-100-fs pulses. [S0031-9007(99)09079-1]

PACS numbers: 72.20.Jv, 61.80.Ba, 77.22.Jp, 79.20.Ds

Laser damage is one of the limiting factors of the transmission and deposition of laser energy in solids. The mechanisms of laser damage are of great importance to the development of high-intensity lasers. In addition, short pulses produce damage with smaller statistical uncertainty in damage threshold than long pulses. Since the discovery of this deterministic feature for short-pulse damage, many practical applications of femtosecond lasers have been developed in areas involving material removal with submicron precision, such as micromachining, ophthalmic surgery, electronics, data storage, and drug release. A large number of experimental and theoretical studies have been conducted to determine the mechanisms of laser damage. However, theoretical models only yield partially satisfactory agreement with experimental observations. Laser damage on short time scales remains an active area of research.

Damage in transparent materials is associated with rapid buildup of conduction electrons to a critical density, which is necessary for further absorption of laser energy. For long pulses, electrons are generated by background carrier seeded impact ionization leading to electron avalanche [1,2]. The background electron density in the conduction band can surpass $10^8\ \mathrm{cm}^{-3}$ in ultrapure crystals at room temperature. With a decrease in the pulse duration, electrons generated by photoionization, such as multiphoton ionization and tunnel ionization, become more appreciable than background carriers for an avalanche to develop.

The availability of ultrafast sub-50-fs lasers and the technology of chirped-pulse amplification [3] have extended the study of laser damage to ultrashort time scales. Du *et al.* [4] reported two remarkable features of ultrashort pulse-induced damage. First, short-pulse damage exhibits deterministic nature as opposed to the statistical behavior for long-pulse damage. Second, as shown in Fig. 1(a), the damage threshold fluence is higher than the prediction from the $\sqrt{\tau}$ scaling rule for pulse duration τ below 10 ps. This is surprising, since the enhancement of multiphoton ionization or other nonlinear effects were expected to reduce the damage threshold from the scaling rule for short pulses. Later, Stuart *et al.* [5], Fig. 1(b), Varel *et al.* [6], Lenzner *et al.* [7], Fig. 1(c), and our recent measurement, Fig. 1(d), confirmed the departure from the scaling rule. However, as depicted in Fig. 1, these measurements have shown different dependence of damage threshold on pulse duration in the subpicosecond regime, but none of the theoretical models [4,5,8,9] proposed before can explain this dissimilarity. In this paper, we present experimental results of single-shot damage threshold measurement. In addition, we develop a theoretical model, with which the conflicting experimental observations can be resolved.

The discrepancy in the experimental results was thought to arise from different experimental conditions. Du *et al.* [4] measured plasma emission from the focal region in the sample to detect damage from a single laser pulse centered at 780 nm. On the other hand, Stuart *et al.* [5] used 1053-nm laser pulses under a multiple-shot condition, 600 shots at 10 Hz, and they defined damage to be any visible permanent modification to the sample with a Nomarski microscope. Varel *et al.* [6] measured the damage threshold with a Nomarski microscope and the threshold for plasma emission under both single-shot and five-shot (at 50 Hz) conditions for laser pulses at 790 nm ranging from 190 fs to 4.5 ps. Varel *et al.* concluded that the damage thresholds obtained with a Nomarski microscope from the single-shot measurement are slightly higher than those from the five-shot measurement. These five-shot results are about a factor of 2 higher than the 600-shot results given by Stuart *et al.* with the same detection method (Nomarski microscopy). Furthermore, the plasma-emission threshold measurement by Varel *et al.* shows that the values from the five-shot measurement are significantly lower than those from the single-shot measurement. These findings imply that the sample may suffer a cumulative change in the material properties as the sample is subjected to a series of subthreshold pulses [2]. In order to study intrinsic laser damage, and to exclude the complexity of cumulative effects, our recent measurement, shown in Fig. 1(d), was done under a single-shot condition. The laser system for the measurement is described in Ref. [10]. The damage was determined with a Nomarski microscope. Only entrance-surface damage was considered in the subpicosecond regime. Self-focusing effects can be neglected

0031-9007/99/82(19)/3883(4)$15.00

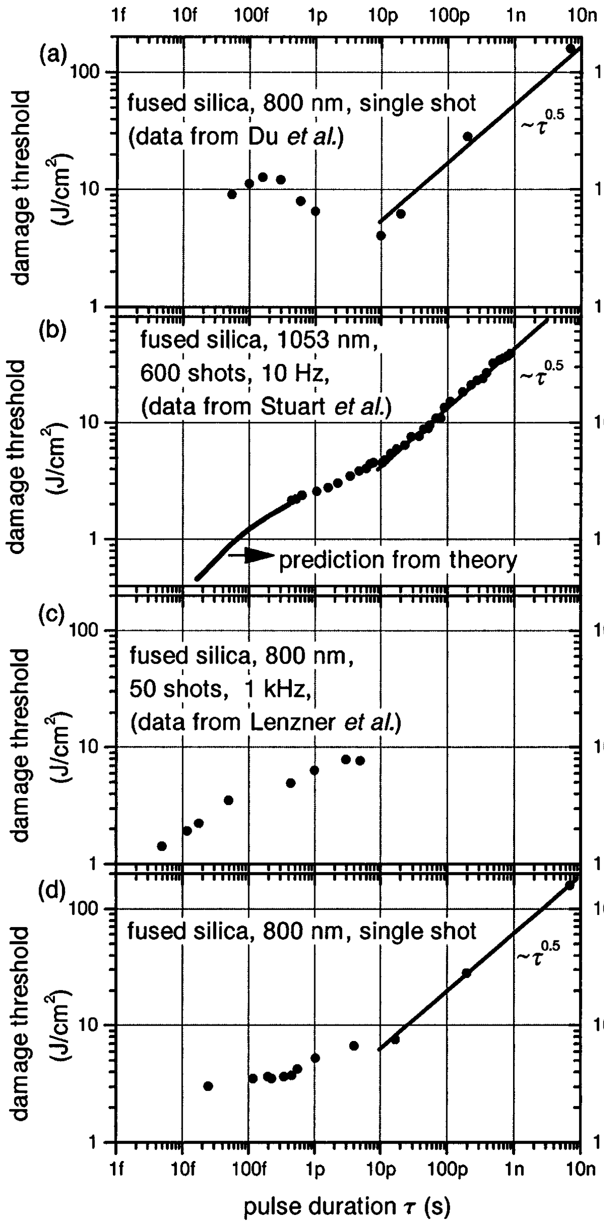

FIG. 1. Damage threshold for fused silica from various groups. Curve (a) is from Du *et al.* [8], who first reported the departure from the $\sqrt{\tau}$ scaling rule for $\tau < 10$ ps. Curve (b) is from Stuart *et al.* [5]. The solid line in the short-pulse regime is the damage threshold predicted by the model described in Refs. [5,9]. Curve (c) is from Lenzner *et al.* [7], who measured the damage fluence for pulses down to 5 fs. Curve (d) is our recent measurement.

in the experiment because of the weak focusing geometry of a ~7-mm confocal range and 150-μm-thick samples.

The dependence of damage threshold on wavelength can be due to the frequency-dependent photoionization rate. For impact-ionization dominated laser damage, the threshold field for damage is lower for longer wavelength due to the nonzero momentum relaxation time [1]. However, since the momentum relaxation time in solids is less than a femtosecond, which is shorter than an optical cycle in the visible range, the damage threshold is nearly independent of the wavelength in the case of avalanche-dominated damage. In contrast, when the pulse duration becomes shorter and multiphoton ionization becomes more important, shorter wavelengths have higher electron yields than longer wavelengths. When the pulse duration is extremely short, where the electric field is extremely high, tunnel ionization should be considered instead of multiphoton ionization. In the tunnel-ionization regime, the dependence of damage threshold on wavelength becomes weak again.

A rate equation approach is commonly used to predict the evolution of the conduction electron density ρ

$$\frac{\partial \rho}{\partial t} = \eta(E)\rho + w_{\mathrm{PI}}(E), \tag{1}$$

where E is the electric field, $\eta(E)$ is the electron avalanche rate, and $w_{\mathrm{PI}}(E)$ is the photoionization rate. The loss term due to electron diffusion and recombination is neglected in Eq. (1) for $\tau \lesssim 10$ ps. Stuart *et al.* [9] suggested linear scaling of the avalanche rate with laser intensity. The resulting model fails to explain the increase in damage threshold fluence F_{th} with decreasing pulse duration for $\tau \lesssim 1$ ps observed by Du *et al.* [4,8]. The photoionization rate used in the calculation from Stuart *et al.* [5,9] and Lenzner *et al.* [7] is based on multiphoton absorption, or $w_{\mathrm{PI}} \propto |E|^{2N}$, where N is the number of photons required to bridge the band gap. Researchers from both groups also point out that the multiphoton ionization term should be replaced by the tunnel ionization expression in a field stronger than ~100 MV/cm. In addition, Lenzner *et al.* [7] report that the prediction from Keldysh's multiphoton absorption theory, which is the low-field limiting version of Keldysh's photoionization theory [11], is orders of magnitude greater than their observed photoionization rate. This could be explained by collision-suppressed ionization rate as suggested by Du *et al.* [8]. Nevertheless, calculations including tunnel ionization have not been presented.

For the avalanche rate $\eta(E)$ in Eq. (1), we will use an expression based on Thornber's model for impact ionization [12]:

$$\eta(E) = \frac{v_s e E}{\Delta} \exp\left\{-\frac{E_I}{E(1 + E/E_{\mathrm{phonon}}) + E_{kT}}\right\}, \tag{2}$$

where v_s is the saturation drift velocity ($\sim 2 \times 10^7$ cm/s), e is the electron charge, Δ is the band gap energy, E_I, E_{phonon}, and $E_{kT} \equiv E_I kT/\Delta$ are the fields for carriers to overcome the decelerating effects of ionization scattering, optical phonon scattering, and thermal scattering in one mean free path, respectively. Du *et al.* [4] also used Thornber's model for the avalanche rate in their calculation. Thornber's formula, plotted in Fig. 2(a), predicts an avalanche rate which scales linearly with the electric field in the strong-field limit. This behavior accounts for the increase of F_{th} with decreasing

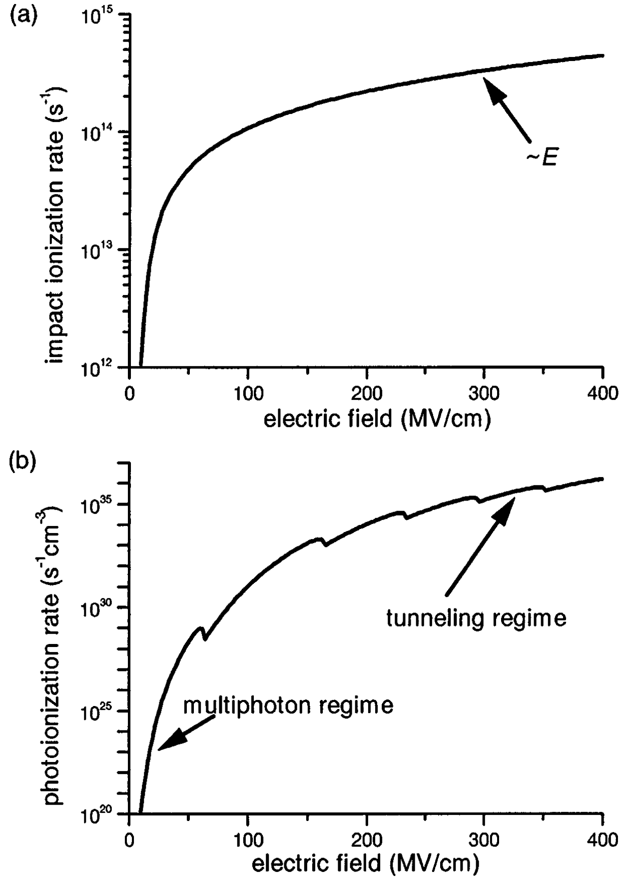

FIG. 2. (a) Impact ionization rate based on Thornber's formula [12]. (b) Typical photoionization rate in solids as predicted by Keldysh's model [11].

τ for $\tau < 1$ ps observed by Du *et al.* [4,8]. They also suggested that multiphoton ionization is strongly suppressed by frequent collisions due to high carrier density. Multiphoton ionization only generates the electrons to seed avalanche.

For the photoionization rate $w_{\mathrm{PI}}(E)$ in Eq. (1), we use Keldysh's calculation for crystals [11]:

$$w_{\mathrm{PI}}(E) = \frac{2\omega}{9\pi}\left(\frac{\omega m}{\sqrt{\gamma_1}\hbar}\right)^{3/2} Q(\gamma, x) \times \exp\left\{-\pi\langle x + 1\rangle \frac{\mathcal{K}(\gamma_1) - \mathcal{E}(\gamma_1)}{\mathcal{E}(\gamma_2)}\right\}, \quad (3)$$

where the definitions of various quantities are listed in Table I. In the case of low frequencies and strong fields ($\gamma \ll 1$), the photoionization rate reduces to the formula for the tunnel effect, while in the opposite limiting case ($\gamma \gg 1$), the ionization rate describes the probability for multiphoton absorption. In other words, Keldysh's photoionization rate asymptotically approaches multiphoton ionization and tunnel ionization at the two extreme limits of the field as might be expected from an analogy with the atomic case. Figure 2(b) shows the general trend for the photoionization rate as a function of electric field. It is worth noting that the adiabatic parameter γ (also known as Keldysh's parameter, defined in Table I) differs from the definition used in gases by a factor of $1/\sqrt{2}$. Moreover, γ can be further reduced since the effective electron mass in solids is normally smaller than the mass of a free electron. Therefore, it seems "easier" to approach the tunnel ionization regime in solids than in atoms. This could be the reason why the observed photoionization rate is orders of magnitude smaller than that estimated by the multiphoton absorption theory.

TABLE I. Definitions of the quantities used in Eq. (3).

ω: laser frequency
$m = \frac{m_e m_h}{m_e + m_h}$: reduced mass of the electron and the hole
$\gamma = \frac{\omega\sqrt{m\Delta}}{eE}$: Keldysh's parameter in solids
$\gamma_1 = \frac{\gamma^2}{1+\gamma^2}$, $\gamma_2 = 1 - \gamma_1 = \frac{1}{1+\gamma^2}$
$Q(\gamma, x) = \sqrt{\frac{\pi}{2\mathcal{K}(\gamma_2)}} \times \sum_{n=0}^{\infty} \exp\left\{-n\pi \frac{\mathcal{K}(\gamma_2) - \mathcal{E}(\gamma_2)}{\mathcal{E}(\gamma_1)}\right\} \Phi\left\{\frac{\pi}{2}\sqrt{\frac{(2\langle x+1\rangle - 2x + n)}{\mathcal{K}(\gamma_2)\mathcal{E}(\gamma_2)}}\right\}$
$x = \frac{2}{\pi}\frac{\Delta}{\hbar\omega}\frac{\sqrt{1+\gamma^2}}{\gamma}\mathcal{E}\left(\frac{1}{1+\gamma^2}\right)$
$\Phi(z) = \int_0^z \exp(y^2 - z^2)\, dy$
$\mathcal{K}$, $\mathcal{E}$: complete elliptic integral of the first and second kinds
$\langle z\rangle$: the integer part of the number z

As for impact ionization, the applicability of an avalanche rate linearly scaled with laser intensity is doubtful. The linear relationship between the avalanche rate and the laser intensity is the consequence of two major assumptions: (1) flux doubling, and (2) unchanged shape of electron distribution [9]. The first assumption means that as soon as the electron reaches an energy sufficient to ionize, a second electron is generated by impact ionization, and both electrons are left at zero energy. The second assumption states that during the avalanche, the energy distribution of the electrons grows in magnitude without changing shape. However, studies based on Monte Carlo methods conclude that in both semiconductors [13] and wide-gap materials [14,15], the shape of the electron distribution is a function of the electric field and electrons can be found with energy greater than the ionization energy. Higher fields cause longer high-energy tails in the electron distribution. Therefore, the two assumptions are violated in a strong electric field.

In our calculation, Thornber's expression, Eq. (2), for impact ionization combined with Keldysh's photoionization rate, Eq. (3), is used to integrate the rate equation, Eq. (1), to obtain the conduction electron density at the end of a laser pulse. The criterion of using the critical plasma density (1.6×10^{21} cm^3 for a laser wavelength of 800 nm) as the onset of damage for electron generation is commonly accepted [4,5,7,9], because the material becomes highly absorbing when the free electron density exceeds the critical plasma density. Therefore,

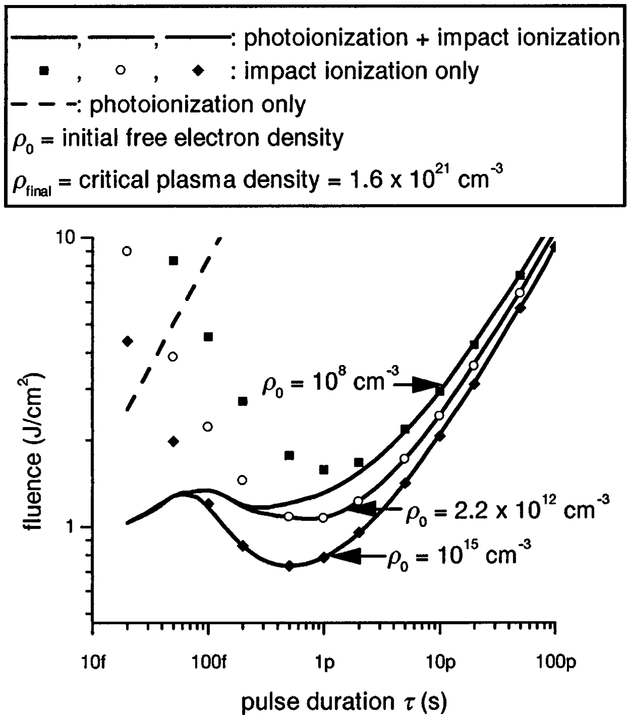

FIG. 3. Damage threshold calculated from solving the rate equation for electron generation Eq. (1) where the threshold electron density is defined as the critical plasma density. The rates for impact ionization and photoionization are based on the expressions from Thornber and Keldysh, Eqs. (2) and (3), respectively. Calculated results from three different initial free electron densities are presented.

this criterion determines the damage threshold. Figure 3 shows the calculated damage threshold fluences derived from different initial free electron densities. Three cases of carrier generation, photoionization only, impact ionization only, and a process including both photoionization and impact ionization, are assumed in the calculation. For long pulses, the damage is governed by impact ionization, while in the case of short pulses, the damage is still done by avalanche but with the assistance of photoionization. For instance, for a 20-fs pulse, the contribution from avalanche becomes much greater than that from photoionization after the free electron density exceeds about 1% of the critical density. Three different initial electron densities are used in the calculation results displayed in Fig. 3. When the initial electron density is high, the reduction of damage threshold due to photoionization is less important, because the initial electron density is high enough for electron multiplication to be the dominant generation process. In other words, a high density of initial electrons, which can be originated from impurities or generated by the pedestal energy in a laser pulse, can mask the effect of photoionization. This could be responsible for the increase in F_{th} with decreasing τ for $\tau \lesssim 1$ ps observed by Du *et al.* [4,8].

In conclusion, we measured the single-shot damage threshold as a function of pulse width down to 20 fs. In addition, we found that in the rate equation approach of laser damage in dielectrics, Thornber's expression for impact ionization and Keldysh's photoionization theory in solids describe the physical processes in the entire optical field range better than the linear scaling of avalanche rate with intensity and multiphoton absorption approximation. Our calculation exhibits the sensitivity of damage threshold to the initial carrier density. The discrepancy found in damage-threshold measurements can be qualitatively explained by our model.

The authors gratefully acknowledge support from the National Science Foundation. The authors also thank Dr. B. Stuart and Dr. M. Lenzner for permission to use their data.

[1] N. Bloembergen, IEEE J. Quantum Electron. **QE-10**, 375 (1974).
[2] S. Jones, P. Braunlich, R. Casper, X. Shen, and P. Kelly, Opt. Eng. **28**, 1039 (1989).
[3] D. Strickland and G. Mourou, Opt. Commun. **56**, 219 (1985).
[4] D. Du, X. Liu, G. Korn, J. Squire, and G. Mourou, Appl. Phys. Lett. **64**, 3071 (1994).
[5] B. Stuart, M. Feit, A. Rubenchik, B. Shore, and M. Perry, Phys. Rev. Lett. **74**, 2248 (1995).
[6] H. Varel, D. Ashkenasi, A. Rosenfeld, R. Herrmann, F. Noack, and E. Campbell, Appl. Phys. A **62**, 293 (1996).
[7] M. Lenzner, J. Krüger, S. Sartania, Z. Cheng, Ch. Spielmann, G. Mourou, W. Kautek, and F. Krausz, Phys. Rev. Lett. **80**, 4076 (1998).
[8] D. Du, X. Liu, and G. Mourou, Appl. Phys. B **63**, 617 (1996).
[9] B. Stuart, M. Feit, S. Herman, A. Rubenchik, B. Shore, and M. Perry, J. Opt. Soc. Am. B **13**, 459 (1996); B. Stuart, M. Feit, S. Herman, A. Rubenchik, B. Shore, and M. Perry, Phys. Rev. B **53**, 1749 (1996).
[10] S. Backus, C. G. Durfee III, G. Mourou, H. C. Kapteyn, and M. M. Murnane, Opt. Lett. **22**, 1256 (1997).
[11] L. V. Keldysh, Sov. Phys. JETP **20**, 1307 (1965).
[12] K. K. Thornber, J. Appl. Phys. **52**, 279 (1981).
[13] K. Yeom, H. Jiang, and J. Singh, J. Appl. Phys. **81**, 1807 (1997).
[14] D. Arnold and E. Cartier, Phys. Rev. B **46**, 15 102 (1992).
[15] D. Arnold, E. Cartier, and D. J. DiMaria, Phys. Rev. B **49**, 10 278 (1994).